# Friction in strongly confined polymer melts: Effect of polymer bridges

A. Subbotin*
*Institute of Petrochemical Synthesis, Russian Academy of Science, Moscow 117912, Russia*

A. Semenov
*Department of Applied Mathematics, University of Leeds, Leeds, United Kingdom*

M. Doi
*Department of Applied Physics, Nagoya University, Nagoya, Japan*
(Received 22 August 1996)

We propose a molecular theory of friction in confined polymer melts between atomically smooth surfaces, taking polymer bridges between the surfaces into account. Using the activation friction model, we consider the bridge adsorption-desorption dynamics and calculate the macroscopic friction force (the tangential stress) in the system as a function of the imposed velocity. We show that the bridges result in the regime where the friction force decreases with the increase of the imposed velocity. The friction force passes through maximum and minimum values in the crossover range between linear and nonlinear regimes. We also investigate the stability of sliding in the regime with decreasing friction force. [S1063-651X(97)09606-2]

PACS number(s): 36.20.−r

## I. INTRODUCTION

Rheology of polymer liquids strongly confined in a nanogap region between two walls is substantially different from that of bulk polymer liquids in many respects [1–14]. The direct measurements of the rheological functions under oscillatory shear demonstrated that the confined liquids exhibit a solidlike behavior for a small amplitude of deformation and liquidlike behavior for a large amplitude [5–7]. In the liquidlike regime, the friction force behavior is rather complicated and depends on the thickness of the polymer film: Shear thinning has been found in the experiments [2,4–7,13,14]. Sometimes the sliding is evinced in the form of stick-slip motion [1,11–13].

The measurements of the linear viscoelasticity under oscillatory shear [5,10] indicated that the loss modulus of confined polymers has a shape characteristic of entangled polymers [15] even though the loss modulus of the same polymer in the bulk state does not show any indication of entanglements. The possible interpretation of this phenomena is that entanglement interactions are enhanced in the confined state [5,10]. However, recent computer simulations [16] demonstrate that the entanglements cannot be induced or enhanced by the restricted geometry. Alternatively, the computer simulations [17–21] suggest that the polymer-surface interactions can be the dominant factor in the rheology of confined systems. These interactions include the short-range forces between the surfaces and the polymer segments, and long-range dispersion forces [22]. These forces can be responsible for the suppression of the mobility of the polymer segments at the surfaces and even result in the formation of an immobilized glassy layer at the surfaces. Straightforward incorporation of the polymer-surface interactions into the model is a very complicated problem.

Recently we have proposed a simple model, which is based on the continuum medium approximation. In this model the polymer-surface interaction is accounted for by two friction coefficients [23,24]: One friction coefficient $\zeta_1$ characterizes the mobility of segments in the adsorbed surface layer of thickness of the order of the segment size $a$ and the second friction coefficient $\zeta_0$ is outside this layer. One of the basic points of this model is the estimation of the desorption time of the chain section of $g$ segments $\tau(g)$. Taking into account that the chain conformation in the melt state is Gaussian [25], and therefore that the chain section has of order $g^{1/2}$ adsorbed segments, the total friction coefficient of the section can be written as $\zeta \sim \zeta_0(g-g^{1/2})+\zeta_1 g^{1/2}$. The desorption time is thus the displacement time on a distance of order $ag^{1/2}$: $\tau(g) \sim a^2 g \zeta$. Assuming that the polymer chains bridge the surfaces, the model qualitatively explains some features of the confined polymer melts. In particular the transition from the solidlike state to the liquidlike state can be attributed to the onset of the bridge breakage process and the existence of two relaxational zones is connected with the contributions of the bridges and loops.

In the present paper we propose a theory of friction in strongly confined polymer liquids that is based on a detailed consideration of the adsorption-desorption dynamics. We thus reconsider the estimation for the chain adsorption-desorption time adopted in the previous work [23]. We also employ the activation model of friction [26], which seems to be more appropriate for the description of nonlinear regimes.

## II. MODEL

We consider the polymer melt confined between two parallel walls that strongly adsorb polymers. We assume that the polymer chains consist of $N$ links (segments) of length $a$ and volume $v$. The chain contour length is $R_{\max} \sim aN$. The thickness of the confined polymer film $h$ is assumed to be smaller than or of the same order as the size of the chain coils

*Author to whom correspondence should be addressed.

 

$h \leqslant aN^{1/2}$. The interaction between the polymer and the wall is characterized by some energy of attraction $-\epsilon$ (the energy of a polymer segment when it is adsorbed on the surface). However, this energy $\epsilon$ does not affect the equilibrium properties of the polymer melt since the interactions are screened in the melt and the correlation length is of the order of the segment size $a$ [25].

The attraction between the polymer and wall affects the dynamics: If the polymer is strongly adsorbed on the surface, the desorption hardly takes place. This effect is not represented by the energy $\epsilon$, but by the activation energy. In order to specify the dynamics, we employ the activation model [26]. We assume that each polymer segment exchanges its position with one of its neighbors by some activation process. The activation energy $U_1$ of a polymer segment adsorbed on the surface is higher than the activation energy $U_0$ of a polymer segment in the bulk. Thus the mean time that the polymer segment stays at its own position is written as [26]

$$\tau_1 = \tau^* \exp\left(\frac{U_1}{k_B T}\right), \quad \tau_0 = \tau^* \exp\left(\frac{U_0}{k_B T}\right), \tag{1}$$

where $\tau^*$ is the characteristic time of molecular oscillations

$$\tau^* \sim a(m/k_B T)^{1/2} \tag{2}$$

and $m$ is the mass of a segment.

According to the above activation model, the diffusion constant of the adsorbed segment $a^2/\tau_1$ is much smaller than that of the bulk liquid $a^2/\tau_0$. Alternatively, one can visualize this in such a way that the polymer segment sitting in the adsorbed layer is surrounded by a very viscous medium and has an effective friction coefficient $\zeta_1 \simeq k_B T \tau_1 / a^2$ that is much larger than that in the bulk state $\zeta_0 \simeq k_B T \tau_0 / a^2$.

The effective friction model implies that if a polymer segment adsorbed on the wall is subjected to an external force $\mathbf{f}$, it moves with the mean velocity $\mathbf{u} = \mathbf{f}/\zeta_1$. This relation, however, is valid only for $f < k_B T/a$. If the force becomes larger, we have to take into account the activation process underlying the motion of the segments. This is done as follows. If the segment is subject to a force $\mathbf{f}$, the activation energy it has to overcome when it moves in the direction $\mathbf{n}$ ($\mathbf{n}$ being a unit vector) is $U_1 - a\mathbf{n}\cdot\mathbf{f}$. Thus the relaxation time is given by [27]

$$\tau_1(\mathbf{n}) = \tau^* \exp\left(\frac{U_1 - a\mathbf{f}\cdot\mathbf{n}}{k_B T}\right), \tag{3}$$

where we assume that $af < U_1$. The average segment velocity $\mathbf{u}$ thus can be found from

$$\mathbf{u} = \left\langle \frac{a\mathbf{n}}{\tau_1(\mathbf{n})} \right\rangle = \frac{a}{\tau_1} \left\langle \mathbf{n} \exp\left(\frac{a\mathbf{f}\cdot\mathbf{n}}{k_B T}\right) \right\rangle, \tag{4}$$

where $\langle\ \rangle$ denotes averaging over the directions $\mathbf{n}$. Here we can separate two cases. (i) $f < (k_B T)/a$ or $u < a/\tau_1$, using the perturbation scheme, we obtain the linear relation between the force and the average velocity $u$, $f \sim \zeta_1 u$, where $\zeta_1 = (k_B T)\tau_1/a^2$. This agrees with the effective friction model. (ii) For $k_B T/a < f < U_1/a$ or $a/\tau_1 < u < a/\tau^*$, with Eq. (4), we find

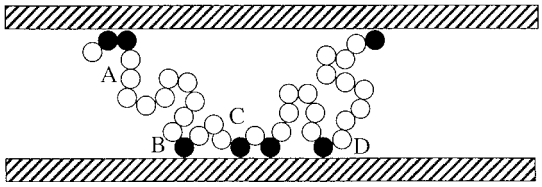


FIG. 1. Typical chain conformation with adsorbed segments. Filled circles imply adsorbed segments and empty circles imply free segments. $AB$ is a bridge, $BC$ is a loop, and $BD$ is an attached section.

$$f \sim \frac{k_B T}{a} \ln\left(\frac{u\tau_1}{a}\right). \tag{5}$$

Thus, in the nonlinear case we obtain a logarithmic dependence of the friction force over the velocity.

## III. EQUILIBRIUM PROPERTIES AND DYNAMICS OF BRIDGES WITH NO FLOW

The typical conformation of a chain confined between two walls consists of *bridges*, which start at one surface and end at another surface, and *attached sections*, which have contacts with only one of the surfaces (Fig. 1). An attached section includes series of *loops* and separates two seccesive bridges. We classify the attached sections according to the number of loops. We consider one of the bridge ends (say, $B$, Fig. 1) and follow the chain configuration until we come to the next contact ($C$) with one of the surfaces. Most probably this is again a contact with the same surface, so that the fragment $BC$ forms a loop with high probability $1-w$. Here $w$ is the small probability that the $BC$ fragment is bridging two surfaces. The length of the bridging fragment must be of order $g_0 \simeq (h/a)^2$, so that $w$ can be roughly interpreted as the probability that a Gaussian polymer fragment, consisting of $g_0$ segments, starts at a surface and does not touch this surface again. Hence $w \sim g_0^{-1/2}$ [28]. As correlations are screened out in the melt state, the probability that an attached section consists of $n$ loops is

$$p_n = w(1-w)^n \sim g_0^{-1/2} \exp(-n/g_0^{1/2}). \tag{6}$$

The average number of contacts per attached section is $\overline{n} = \Sigma n p_n \sim g_0^{1/2}$.

The $n$ loops in the attached section between the succesive bridging fragments can be also considered an *attached blob* with $g$ links. Gaussian statistics implies that

$$n \simeq g^{1/2}. \tag{7}$$

The surface concentration of the bridges and attached sections is [23]

$$\nu_0 \simeq h/v g_0 \simeq a^2/vh; \tag{8}$$

therefore the surface concentration of attached sections, consisting of $g$ segments, is

$$\nu(g) \sim \nu_0 n p_n \sim (a/v)(a/h)^2 g^{1/2} \exp[-(g/g_0)^{1/2}]. \tag{9}$$

Obviously the number of contacts $n$ and the length $g$ of an attached blob are fluctuating. Any particular blob would disappear (detach from the surface) during a characteristic time $\tau(g)$. For $g=1$ this is the relaxation time of one segment $\tau(1)\sim\tau_1$. Since the adsorption-desorption process is determined by the time $\tau_1$, it is natural to assume a scaling law $\tau(g)\sim\tau_1 g^x$. When a typical blob of size $g_0$ is detaching, the fraction of time it spends in the state with one contact $(n=1)$ is $p\sim\tau(1)/\tau(g_0)\sim g_0^{-x}$. On the other hand, this quantity can be found from the equilibrium bridge statistics: $p\sim\nu(1)/\nu(g_0)\sim g_0^{-1/2}$. Therefore, $x=\frac{1}{2}$ and

$$\tau(g)\sim\tau_1 g^{1/2}. \tag{10}$$

We thus conclude that the adsorption-desorption time of a typical bridge is

$$T_1\sim\tau(g_0)\sim\tau_1 g_0^{1/2}. \tag{11}$$

The bridges and loops dynamics away from the surfaces is governed by the Rouse time $T_0\sim\tau_0 g_0^2$. The surface effects become dominant when $T_1>T_0$ or $\tau_1/\tau_0>(h/a)^3$. Below we assume that this condition is fulfilled.

## IV. LINEAR REGIME

Shear flow is imposed by moving one of the surfaces with respect to the other one with a constant velocity $u$. A slow enough flow does not affect the adsorption-desorption dynamics of the bridges. During the time interval $\sim T_1$ the bridge attains maximum elongation force in the tangential direction

$$F_t\sim(k_BT/g_0a^2)(uT_1)\sim u\zeta_1(a/h). \tag{12}$$

After that it detaches by random diffusion and transforms to a loop.

The shear stress (the friction force per unit area) has two contributions: One arises from the bridges and the other from the loops (or attached sections). The contribution from the bridges can be estimated by the product of the bridge elongation force (the tangential component of this force) and the surface concentration of the bridges

$$\sigma_1\sim\nu(g_0)F_t\sim a^3u\zeta_1/h^2v. \tag{13}$$

The stress linearly depends on the imposed velocity, as it should be in the linear regime. It increases with increasing surface friction, $\zeta_1$ and decreases with increasing distance $h$ between the surfaces.

The second contribution from the loops has been calculated in [23], it is equal to the product of the surface concentration of the attached sections, which is equal to the concentration of bridges $\sim\nu_0$ and the elongation force per attached section $F_{tt}\sim u\zeta_0 g_0$,

$$\sigma_0\sim\nu_0F_{tt}\sim hu\zeta_0/v. \tag{14}$$

The bridge contribution to the stress is dominant when $\sigma_1>\sigma_0$ or $\zeta_1/\zeta_0>(h/a)^3$. This condition coincides with the condition that the adsorption-desorption time $T_1$ exceeds the Rouse time $T_0$. The linear regime (regime 1) is limited by the condition that a bridge does not attain maximum elongation $\sim ag_0$ during the time $T_1$: $uT_1<ag_0$ or $u<u_1$, where

$$u_1=ag_0/T_1\sim h/\tau_1. \tag{15}$$

## V. NONLINEAR REGIME

When the imposed velocity $u>u_1$ the behavior becomes more complicated. The maximum blob, containing $g_0$ segments, cannot be attached to the surface during the bridge elongation time [23,24]

$$t^*\sim ag_0/u. \tag{16}$$

The characteristic blob of $g$ segments, which is attached to the adsorbed surface layer during the elongation time, is determined by the condition $\tau_1 g^{1/2}\sim t^*$:

$$g\sim(t^*/\tau_1)^2\sim(h^2/au\tau_1)^2. \tag{17}$$

The bridge concentration $\nu$ can be found using Eq. (9):

$$\nu\sim\nu(g)\sim(a/v)\,\frac{a}{u\tau_1}. \tag{18}$$

If the imposed velocity $u>u_2$, where

$$u_2\sim(h/a)^2(a/\tau_1), \tag{19}$$

then Eq. (17) formally implies that $g<1$. Physically, this means that a segment once attached to a surface would be readily detached during a time shorter than $\tau_1$. Let us find the bridge concentration in the regime $u>u_2$. While the bridges are being created from (large) loops the rate of formation of contacts is not essentially affected by the flow if the flow does not perturb the loop statistics in the direction normal to the surfaces. (The flow does affect the loops significantly if $u>u_4\sim(a/\tau_0)(a/h)^2$ [see Eq. (28)]; we assume here that $u_4\gg u_2$, i.e., that $\tau_1/\tau_0\gg(h/a)^4$.) On the other hand, the rate of bridge detachment is proportional to $1/t^*$. A detailed balance between the formation and detachment of the bridges thus imply that $\nu\propto t^*\propto 1/u$ in the region $u>u_2$. Taking into account that for $u\sim u_2$ the concentration of bridges is estimated as $\nu\sim\nu(1)\sim(a/v)(a/h)^2$, we see that $\nu\sim(a/v)(a/u\tau_1)$ in both regimes $u<u_2$ and $u>u_2$. Note that the number of segments in contact with a surface per one attached blob $(g)$ is

$$n\sim g^{1/2}\sim\frac{h^2}{au\tau_1},\quad u<u_2 \tag{20}$$

$$n\sim 1,\quad u>u_2. \tag{21}$$

After a bridge attains the maximum elongation, the segments of the corresponding attached blobs must start to move relative to the surfaces with the tangential velocity $u_t$, which is of order $u$, thus producing a high friction. At the onset of this process, when only one segment is involved in the motion, the friction force is determined by Eq. (5),

$$F_b\sim(k_BT/a)\ln(u\tau_1/a). \tag{22}$$

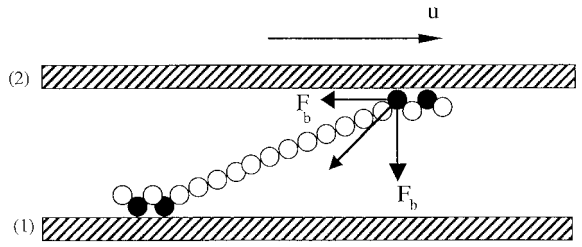


FIG. 2. Local geometry of the forces, acting on the breaking bridge.

In order to calculate the flow-induced detachment time of one segment $\tau_b$, let us consider the local chain conformation (Fig. 2). The segment next to the attached segment along the chain is typically situated in the second surface layer, so that the angle $\alpha$ between the tension force and the surface is of order unity $\alpha \sim 1$. This tensile force drives the attached segment away from the surface with the normal velocity $u_n$, which is of order $u$. Thus the detachment time of one segment is of order

$$\tau_b \sim a/u. \tag{23}$$

Since the attached segments detach independently, the total time during which the high friction force $F_b$ [Eq. (22)] is acting is $n\tau_b$, where $n$ is the number of the attached segments.

Let $F_\tau(t)$ be the tangential component of the bridge elongation force. The average shear stress in the system can be written as

$$\sigma_1 \sim \nu(g) \int_0^{t^*} F_\tau(t)dt/t^* \sim \nu(g)(k_BT/a + n\tau_b F_b/t^*). \tag{24}$$

The first term in this equation is the contribution of the bridges on the elongation stage and the second term is connected with the detaching bridges. Thus we can identify the following two nonlinear regimes.

In regime 2, $u_1 < u < u_2$, the shear stress is defined by Eqs. (18), (20), and (22)–(24),

$$\sigma_1 \sim \frac{k_BT}{v}\left[\frac{a}{u\tau_1} + \left(\frac{a}{u\tau_1}\right)^2 \ln\left(\frac{u\tau_1}{a}\right)\right]. \tag{25}$$

Note that the first term in this equation, which is connected with the elongating bridges, is always dominant. The stress decreases with increasing imposed velocity; therefore, in the crossover range between the linear and nonlinear regimes the stress passes through a maximum.

Regime 3 corresponds to higher velocities $u > u_2$. Using Eq. (21) instead of Eq. (20), we get

$$\sigma_1 \sim \frac{k_BT}{v}\frac{a}{u\tau_1}\left[1 + \left(\frac{a}{h}\right)^2 \ln\left(\frac{u\tau_1}{a}\right)\right]. \tag{26}$$

The first term is still dominant in this regime.

The second contribution to the stress is connected with the flow inside the layer. In the linear regime this stress is defined by Eq. (14). The total stress is therefore the sum of contributions Eqs. (14) and (26).

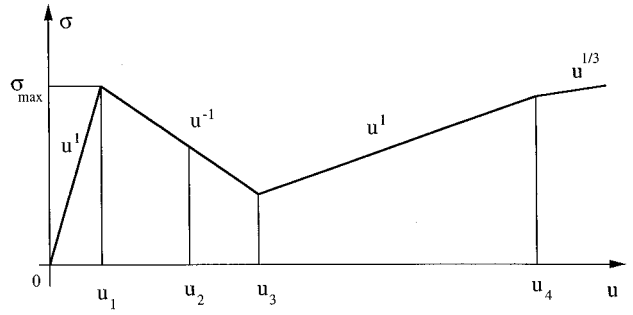


FIG. 3. Plot of the friction force vs the imposed velocity.

This stress passes through a minimum at the velocity

$$u \sim u_3 \sim \frac{a^{3/2}}{(\tau_0\tau_1 h)^{1/2}}. \tag{27}$$

Thus, for the velocities $u < u_3$ the stress is determined by Eq. (26) (regime 3) and for $u > u_3$ the stress is given by Eq. (14) (regime 4).

When the imposed velocity becomes very high so that the bridge elongation time is smaller than the Rouse time $t^* < T_0$, the flow results in a nonlinear loops behavior and a new regime emerges. This regime (regime 5) has been considered in our previous papers [23]. The critical velocity $u_4$ separating this regime from the regime 4 is

$$u_4 \sim (a/\tau_0)(a/h)^2. \tag{28}$$

If $u > u_4$, then the flow suppresses the chain fluctuations in the normal direction, so that the characteristic normal size of this fluctuation becomes of order $a(u\tau_0/h)^{-1/3}$ [23] and the bridges cannot be formed at all. The shear stress in this case is given by

$$\sigma \sim (k_BT/v)(u\tau_0/h)^{1/3}.$$

The power 1/3 in the equation is connected with the finite chain extensibility and incompressibility of the polymer melts and thus is universal if the film thickness is constant. The computer simulations for short-chain molecules predict another power law $\sigma \sim u^{1/2}$ [19–21], which may be connected with some compressibility of the systems.

The plot of the macroscopic friction force versus the imposed velocity is shown in Fig. 3. The stress passes through a maximum at the velocity $u \sim h/\tau_1$ and then decreases over a wide range of imposed velocity. The behavior corresponds to the regimes where the stress is mainly due to the polymer bridges. At high velocities $u > a^{3/2}/(h\tau_0\tau_1)^{1/2}$ the contribution of the loops to the stress become dominant and the stress starts to increase again after passing through a minimum value.

## VI. TRANSIENT REGIMES

In this section we consider the stress behavior after a sliding is applied and then stopped (Fig. 4). If the velocity $u > u_1$ is imposed to a confined melt in equilibrium, then the bridges attain maximum elongation at the time $t^* \sim ag_0/u$. At that moment the shear stress attains the maximum value

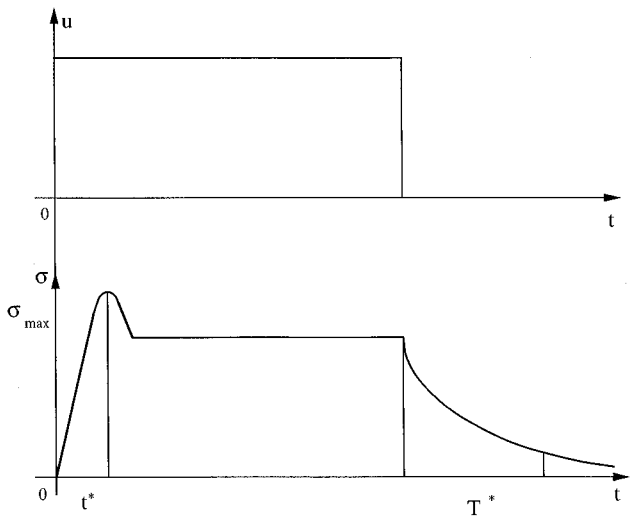


FIG. 4. Plot of the friction force after the sliding has been applied and stopped.

$$\sigma_{\max} \sim (k_B T/v)(a/h). \tag{29}$$

This value does not depend on the imposed velocity and can be attributed to the static friction [1,11,13]. If $\sigma < \sigma_{\max}$, then the stationary sliding velocity is very low $u \sim h/\tau_1$; if $\sigma > \sigma_{\max}$ the velocity increases up to a much higher value $u' \sim a^3/h^2\tau_0$.

We can identify the four stages in the stress relaxation dynamics after stopping the flow. The first stage corresponds to $t < \tau_b$. In this stage the initially stretched bridges break and the stress decreases slightly. In the second stage, which corresponds to the time scale $\tau_b < t < T_1$, the elongated bridges relax. However, the chains continue to be locally stretched in the tangential direction. Their conformation can be described as a random sequence of stretched $g_0$ blobs. The Rouse relaxation time of the chain conformation $T^*$ can be estimated as

$$T^* \sim T_1 (N/g_0)^2 \sim \tau_1 N^2 (a/h)^3, \tag{30}$$

where $T_1$ is the characteristic blob relaxation time [see Eq. (11)] and $N/g_0$ is the number of blobs in the chain.

Thus the third stage corresponds to the time interval $T_1 < t < T^*$. The last stage implies $t > T^*$.

## VII. ANALYSIS OF THE SLIDING STABILITY

According to the classical theory of friction, if the friction force decreases with the increase of the imposed velocity such as in regimes 2 and 3 in our case, an instability of sliding can appear [29–31]. We now analyze this for a typical system used in the friction experiments shown in Fig. 5.

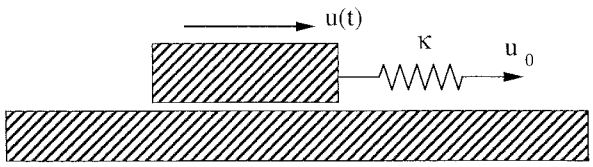


FIG. 5. Schematic geometry of shearing surfaces.

When the sliding velocity $u_0(t)$ is applied to one of the surfaces through the mechanical coupling $\kappa$, this surface slides over the other fixed surface with the velocity $u(t)$, which in general does not coincide with $u_0(t)$. We can describe the coupling in terms of an elastic spring with the elastic constant $\kappa$. If the spring is elongated by $\Delta x$, the elastic stress is changed by $\Delta\sigma = \kappa \Delta x$ (here and in the following we will attribute this stress to the unit area). Omitting the inertial effects, we can connect the time derivative of the stress $d\sigma(t)/dt$ in the system with the velocity difference $u_0(t) - u(t)$:

$$\frac{d\sigma(t)}{dt} = \kappa(u_0(t) - u(t)). \tag{31}$$

At the same time, the stress $\sigma$ is equal to the friction force and is a function of the velocity $u(t)$, $\sigma = \phi(u(t))$. Using Eq. (31), we express $u(t)$ through $u_0$ and $d\sigma/dt$ and get the equation for the stress:

$$\sigma = \phi\left( u_0 - \frac{1}{\kappa}\frac{d\sigma}{dt} \right). \tag{32}$$

If the imposed velocity $u_0$ is constant, the stationary stress $\sigma_0 = \phi(u_0)$ is a solution of Eq. (32).

The stability of the solution under the fluctuations $\sigma' = \sigma - \sigma_0$ can be investigated after an expansion of the function $\phi$ in the vicinity of $u_0$. The corresponding equation for $\sigma'$ in the linear approximation is given by

$$\sigma' = -\lambda(d\sigma'/dt), \tag{33}$$

where

$$\lambda = (1/\kappa)(d\phi/du_0). \tag{34}$$

Obviously, if $\lambda < 0$, which implies that the friction force decreases with increasing velocity, the system is unstable.

Note, however, that Eq. (32) assumes that the relaxational processes in the system occur very fast, i.e., the characteristic relaxation time of the system is much smaller than $\lambda$. In order to take the relaxational processes into account we should present the stress not as a nonlinear function of the velocity, but as a nonlinear functional $\sigma = \Phi[t, u(t)]$. Obviously, for $u = u_0 = \text{const}$, $\Phi[t, u_0] = \phi(u_0)$ and the stress $\sigma = \phi(u_0)$. The stability of the system can be investigated in the usual way after an expansion of the functional $\Phi[t, u(t)]$ in the series at the vicinity of the point $u = u_0$,

$$\Phi[t, u_0 + u'(t)] = \phi(u_0) + \int_{-\infty}^{t} B(t - t' | u_0) u'(t') dt' + \cdots, \tag{35}$$

where $B(t - t' | u_0)$ is the memory function, depending on the nature of the lubricant and the imposed velocity [here $u'(t) = -(1/\kappa)(d\sigma'/dt)$]. The linear equation for the stress $\sigma'$ is given by

$$\sigma' = -\frac{1}{\kappa} \int_{-\infty}^{t} B(t - t' | u_0) \frac{d\sigma'(t')}{dt'} dt'. \tag{36}$$

If $\tau \to 0$, then $B(t-t'|u_0) \to (d\phi/du_0)\delta(t-t')$ and we return to Eq. (33). In the general case Eq. (36) can be simplified if we assume a solution of the form $\sigma' \sim \exp(\alpha t)$,

$$\alpha B^*(\alpha) = -\kappa, \tag{37}$$

where $B^*(\alpha) = \int_0^\infty B(t|u_0)e^{-\alpha t}dt$ is the Laplace transform of the function $B(t)$. If Eq. (37) has a positive solution ($\alpha > 0$), instability takes place. Thus the problem is reduced to the calculation of the memory function $B(t)$. We will derive the corresponding equations for our model.

We have identified two regimes where the friction force decreases with increasing velocity. In the first approximation, the stress in these regimes is determined by the elongating bridges and is given by [see Eqs. (24)–(26)]

$$\sigma(t) \sim \nu(t)(k_B T/a), \tag{38}$$

where $\nu(t)$ is the surface concentration of the bridges at the time $t$. If the velocity $u(t)$ varies slowly with time, the surface bridge concentration is [see Eq. (18)]

$$\nu(u(t)) \sim (a/v)\,\frac{a}{u(t)\tau_1}. \tag{39}$$

However, for an arbitrary velocity, the bridge concentration depends on the flow history and cannot be written in a simple form. The situation is simplified if the velocity perturbation $u'(t) = u(t) - u_0$ is small, $|u'(t)| \ll u_0$. In the first approximation, the equation for the surface bridge concentration is written as the relaxational one [24]

$$t_0^* \frac{d\nu(t)}{dt} = \nu(u(t)) - \nu(t), \tag{40}$$

where the bridge relaxation time $t_0^*$ is the same order of magnitude as the bridge elongation time

$$t_0^* \sim h^2/au_0. \tag{41}$$

Taking the mechanical coupling into account, the equation for the stress is

$$t_0^* \frac{d\sigma(t)}{dt} = \sigma\left(u_0 - \frac{1}{\kappa}\frac{d\sigma}{dt}\right) - \sigma(t). \tag{42}$$

After linearization, we obtain the following equation for the perturbation $\sigma' = \sigma(t) - \sigma(u_0)$:

$$\left(t_0^* - \frac{1}{\kappa}\frac{d\sigma(u_0)}{du_0}\right)\frac{d\sigma'}{dt} = -\sigma'. \tag{43}$$

Instability appears when the term in large parentheses is negative or when the imposed velocity satisfies the condition

$$u_0 < u^* = (\kappa^*/\kappa)(h/\tau_1) \quad \text{where} \quad \kappa^* = (k_B T/vh)(a/h)^2. \tag{44}$$

Thus, if $u^* < u_1$ or $\kappa > \kappa^*$, the sliding is stable in the whole range of the imposed velocity; if $u_1 < u^* < u_3$, instability appears for the velocities $u_1 < u_0 < u^*$; if $u_3 < u^*$, the range of instability is $u_1 < u_0 < u_3$. The diagram of the sliding behavior in the coordinate $(\kappa, u_0)$ is shown in Fig. 6.

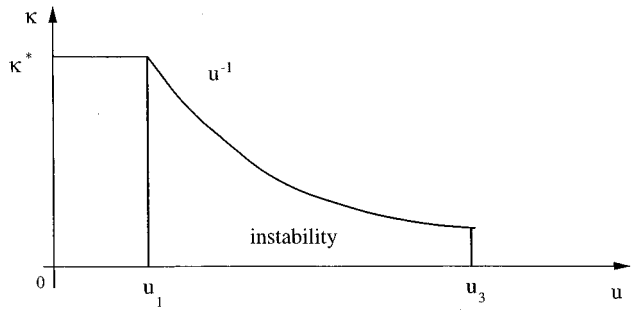


FIG. 6. Diagram of the sliding behavior.

## VIII. STICK-SLIP MOTION

Let us consider sliding in an unstable regime and start with the simplest situation, when the spring elastic constant $\kappa$ is small. As before, we assume that the inertial effects are small. The motion can be understood from Fig. 7. After the stress has been released during the previous cycle of motion and attained the minimum value

$$\sigma_{\min} \sim (k_B T/v)(\tau_0 h/\tau_1 a)^{1/2}, \tag{45}$$

the sliding velocity is close to zero and the bridges start to restore and elongate (point $A$, Fig. 7). The motion following the state at point $A$ can be analyzed as follows. Let $x(t)$ be the mean end-to-end distance of a bridge. The force acting on the top surface by the bridges is $\nu(t)(k_B T/h^2)x(t)$. This has to balance with the mechanical coupling force $\kappa(u_0 t - x(t))$ (the origin of the time is taken at the state $A$). Therefore,

$$\nu(t)(k_B T/h^2)x(t) = \kappa(u_0 t - x(t)), \tag{46}$$

where $\nu(t)$ is the surface bridge concentration at the time $t$. This concentration can be found from Eq. (9), taking into account that characteristic blob of $g(t) \sim (t/\tau_1)^2$ segments is attached to the surface during the time $t$,

$$\nu(t) \sim (a/v)(a/h)^2(t/\tau_1). \tag{47}$$

After $t \sim T_1$ the surface bridge concentration attains the maximum value $\nu_0$ and the distance $x(T_1)$ is

$$x(T_1) \sim hu_0\tau_1/a(1+\kappa^*/\kappa). \tag{48}$$

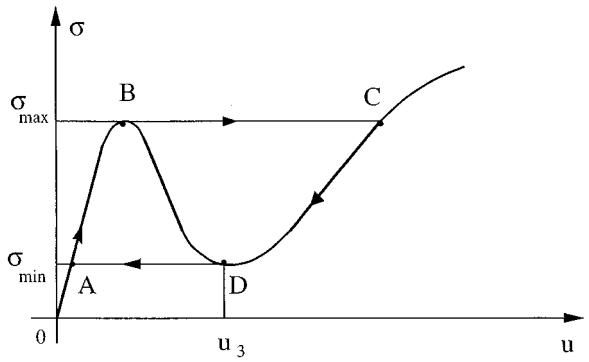


FIG. 7. Transitions in the system during the stick-slip cycle.

$x(T_1)$ is smaller than the maximum bridge length $h^2/a$ if the imposed velocity $u_0 < u^* + u_1$. Since the range of instability is $u_0 < u^*$ [Eq. (44)], the condition $x(T_1) < h^2/a$ is always fulfilled.

After the bridges are restored the stress dynamics can be approximately described by the equation

$$\sigma(t) = a^3 u(t) \zeta_1 / h^2 v = \sigma_{\min} + \kappa u_0 t. \tag{49}$$

This equation implies that the stress that is accommodating in the spring equals the friction force in the linear regime. Obviously the stress can increase up to the yield point ($B$), where it attains the maximum value

$$\sigma_{\max} \sim (k_B T/v)(a/h). \tag{50}$$

The duration of this process is

$$T' \sim (\sigma_{\max} - \sigma_{\min})/\kappa u_0 \sim (h^2/a u_0)(\kappa^*/\kappa). \tag{51}$$

After the transition through the yield point the velocity cannot continuously increase anymore because the friction force decreases in this case. The only possibility for the system is to transform to the point $C$ with breakage the bridges. The velocity sharply increases at the moment and the effective layer viscosity sharply decreases. Therefore, the stress is released very quickly and decays to the minimum value $\sigma_{\min}$ (point $D$) in the time of the order of Rouse time $T_0 \sim \tau_0 (h/a)^4$. At the point $D$, the velocity again cannot decrease continuously because in this case the friction force increases and the spring elastic force decreases. Thus the velocity decreases sharply and system transforms to the initial point $A$ and the cycle is repeated.

According to this picture, stick slip occurs as a periodic transition between two states, which can be associated with solidlike and liquidlike states. In the solidlike state the surface bridges concentration coincides with the equilibrium one and the stress increases linearly with the imposed velocity. After the yield point is attained, the bridges are broken and the system transforms to the liquidlike state. In this state the stress is released. The maximum and the minimum stress values in this cycle do not depend on the imposed velocity.

## IX. DISCUSSION AND CONCLUSION

In the present paper we have developed nonlinear theory of friction in strongly confined polymer liquids. We assumed that the polymer segments in the adsorbed surface layer have a very small mobility and showed that rheology of the confined polymer melts is dominated by the bridges between the surfaces (except for very high imposed velocity). The relaxation time (the lifetime) of a segment in the adsorbed surface layer $\tau_1$ is much longer than the relaxation time of the segment out of the layer $\tau_0$, $\tau_1 \gg \tau_0$. It was found that adsorption-desorption time $T_1$ of the bridge in the equilibrium is proportional to the number of contacts between the bridge and the surface, i.e., $T_1 \sim \tau_1 g_0^{1/2}$, where $g_0 = (h/a)^2$ is the number of segments in the bridge. This result has been derived from the equilibrium bridge statistics. Other characteristic times of the system are connected with the loops and the chains themselves. The loop relaxation can be described by the Róuse dynamics; therefore, the relaxation time of the loop is $T_0 \sim \tau_0 (h/a)^4$. The relaxation of the chain conformation is determined by the surface friction and the relaxation time is of order $T^* \sim \tau_1 N^2 g_0^{-1/2}$. It depends on the molecular mass of the polymer chains.

In order to describe nonlinear bridge dynamics we employed the idea of activation friction [26]. For a constant imposed velocity $u$ four main regimes in the shear stress have been identified:

$$\begin{aligned} &\sigma \propto u \tau_1 / h^2, \quad u < h/\tau_1 \\ &\sigma \propto 1/u\tau_1, \quad h/\tau_1 < u < a^{3/2}/(h\tau_0\tau_1)^{1/2} \\ &\sigma \propto uh\tau_0, \quad a^{3/2}/(h\tau_0\tau_1)^{1/2} < u < a^3/h^2\tau_0 \\ &\sigma \propto (u\tau_0/h)^{1/3}, \quad u > a^3/h^2\tau_0. \end{aligned} \tag{52}$$

For very small imposed velocities the bridges break thermally and the linear regime is realized. With increasing velocity, the shear stress passes through a maximum and starts to decrease. This behavior arises from the decrease of the surface bridge concentration. In the nonlinear regime the surfaces become effectively repulsive for the bridges and thus result in the decrease of the surface bridge concentration and the stress. Increasing the velocity further the friction due to the flow inside the layer becomes dominant. First the behavior is linear, and after some critical velocity, the nonlinear flow regime is realized where no bridges are formed. In this regime we predict a 1/3 power law for the stress on the imposed velocity.

We also analyzed the stability of sliding in the regime where the friction force decreases with the velocity. Assuming that the driving force is applied through the mechanical coupling (the spring in our case), we demonstrated that the existence of temporary bridges results in an instability of sliding. Three types of system behavior can be identified. The first type implies that the spring elastic constant obeys the condition

$$\kappa < \kappa^* (\tau_0/\tau_1)^{1/2} (h/a)^{3/2}. \tag{53}$$

In this regime stick-slip motion exists for the velocity interval $u_1 < u_0 < u_3$. It can be described in terms of a transition between solidlike and liquidlike states. In the solidlike state the surface bridges concentration coincides with the equilibrium one. In this state the stress increases linearly up to the yield point, where it attains the maximum value $\sigma_{\max} \sim (k_B T/v)(a/h)$ (the static friction force). At this point the bridges are broken and the system transforms to the liquidlike state with low viscosity, where the stress is released and decays to the minimum value $\sigma_{\min} \sim (k_B T/v)(\tau_0 h/\tau_1 a)^{1/2}$ (the kinetic friction force). At this point the sliding velocity decreases sharply and the system returns to the solidlike state again. The static and kinetic friction force do not depend on the imposed velocity. If the velocity $u_0$ is smaller than $u_1$ or higher than $u_3$ the sliding is stable.

The second situation appears when the elastic constant satisfies

$$\kappa^* (\tau_0/\tau_1)^{1/2} (h/a)^{3/2} < \kappa < \kappa^* (a/h). \tag{54}$$

The stick-slip motion appears for the imposed velocity $u_1 < u_0 < u^*$. For the velocity $u_0 > u^*$ the stress first decreases and when $u_0 > u_3$ it starts to increase. The last situation corresponds to

$$\kappa^* < \kappa, \tag{55}$$

where the sliding is always stable.

Our results qualitatively agree with recent experiments on stick-slip motion in confined polymer liquids [1,11,12]. We found that stick-slip motion can be described in terms of the transition between solidlike and liquidlike states and thus our model is close to the phase transition model [1,11,12,32,33].

## ACKNOWLEDGMENTS

This research was supported by Japan Society for the Promotion of Science and by the Netherlands Organization for Scientific Research (NWO) through the Russian-Dutch exchange programs.

[1] M. L. Gee, P. M. McGuiggan, J. Israelachvili, and A. N. Holoma,, J. Chem. Phys. **93**, 1895 (1990).
[2] A. N. Holoma, H. V. Nguyen, and G. Hadziioannou,, J. Chem. Phys. **94**, 2346 (1991).
[3] H. Hu and S. Granick,, Science **258**, 1339 (1991).
[4] S. Granick,, Science **253**, 1339 (1991).
[5] H. Hu, C. Carson, and S. Granick,, Phys. Rev. Lett. **66**, 2758 (1991).
[6] G. Reiter, A. L. Demirel, and S. Granick,, Science **263**, 1741 (1994).
[7] G. Reiter, A. L. Demirel, J. Peanasky, L. L. Cai, and S. Granick,, J. Chem. Phys. **101**, 2606 (1994).
[8] H. Hu and S. Granick,, Langmuir **10**, 3862 (1994).
[9] S. Granick, H. Hu, and C. Carson,, Langmuir **10**, 3867 (1994).
[10] H. Hu, S. Granick, and K. S. Schweizer, J. Non-Cryst. Solids **172**, 721 (1994).
[11] H. Yoshizawa and J. Israelachvili,, J. Phys. Chem. **97**, 11 300 (1993).
[12] H. Yoshizawa, P. McGuiggan, and J. Israelachvili,, Science **259**, 1305 (1993).
[13] S. Hirz, A. Subbotin, C. Frank, and G. Hadziioannou,, Macromolecules **29**, 3970 (1996).
[14] G. Luengo, F. J. Schmitt, and J. Israelachvili (unpublished).
[15] M. Doi and S. F. Edwards, *The Theory of Polymer Dynamics* (Oxford University Press, Oxford, 1986).
[16] J. S. Shaffer,, Macromolecules **29**, 1010 (1996).
[17] I. Bitsanis and J. Pan,, J. Chem. Phys. **99**, 5520 (1993).
[18] G. ten Brinke, D. Ausserre, and G. Hadziioannou,, J. Chem. Phys. **89**, 4374 (1988).
[19] P. A. Tompson, G. S. Grest, and M. O. Robbin,, Phys. Rev. Lett. **68**, 3448 (1992).
[20] E. Manias, A. Subbotin, G. Hadziioanou, and G. ten Brinke, Mol. Phys. **85**, 1017 (1995).
[21] E. Manias, G. Hadziioannou, I. Bitsanis, and G. ten Brinke,, Europhys. Lett. **24**, 99 (1993).
[22] J. N. Israelachvili, *Intermolecular and Surface Forces*, 2nd ed. (Academic, London, 1991).
[23] A. Subbotin, A. Semenov, E. Manias, G. Hadziioannou, and G. ten Brinke,, Macromolecules **28**, 1511 (1995); **28**, 3898 (1995).
[24] A. Subbotin, A. Semenov, G. Hadziioannou, and G. ten Brinke,, Macromolecules **29**, 1296 (1996).
[25] P. G. de Gennes, *Scaling Concepts in Polymer Physics* (Cornell University Press, Ithaca, 1985).
[26] J. Frenkel, *Kinetic Theory of Liquids* (Clarendon, Oxford, 1946).
[27] G. M. Bartenev and V. V. Lavrentyev, *Friction and Wear of Polymers* (Khimiya, Leningrad, 1972).
[28] E. Eisenriegler, *Polymers Near Surfaces* (World Scientific, Singapore, 1993).
[29] E. Rabinowicz, *Friction and Wear of Materials* (Wiley, New York, 1965).
[30] F. P. Bowden and D. Tabor, *Friction and Lubrication*, 2nd ed. (Methuen, London, 1967).
[31] J. M. Carslon and J. S. Langer,, Phys. Rev. A **40**, 6470 (1989).
[32] P. A. Thompson and M. O. Robbins,, Science **250**, 792 (1990).
[33] O. M. Robbins and P. A. Thompson,, Science **253**, 916 (1991).